Generalized Franck-Condon principle for resonant photoemission

Paweł Sałek, Faris Gel'mukhanov,* and Hans Ågren
Division of Theoretical Chemistry, The Royal Institute of Technology, S-10044 Stockholm, Sweden

Olle Björneholm and Svante Svensson
Department of Physics, Uppsala University, Box 530, S-75121 Uppsala, Sweden

(Received 3 May 1999)

A generalized Franck-Condon (GFC) principle for resonant x-ray Raman scattering and for resonant photoemission in particular is derived and numerically investigated. The GFC amplitudes differ from ordinary FC amplitudes by the presence of photon and photoelectron phase factors which describe the coupling—or interference—of the x-ray photons or Auger electrons with the nuclear motion. With the GFC amplitudes, a Kramers-Heisenberg relation is obtained for vibronic transitions that corrects the so-called lifetime-vibrational interference formula. For resonant photoemission in the soft-x-ray region involving typical bound potential surfaces, the generalization gives a contribution to the FC factors that can amount to 20%. For core excitation above the dissociation threshold, the GFC principle relates to Doppler effects on the ejected photoelectron both for the so-called ''molecular'' and ''atomic'' bands. The role of the GFC principle in direct photoionization is briefly discussed. [S1050-2947(99)08809-5]

PACS number(s): 33.60.Fy, 33.20.−t

I. INTRODUCTION

High-resolution dispersive and detector techniques have made it possible to analyze vibrational fine structure in x-ray and Auger emission for almost three decades [1–8]. It was early realized that, contrary to the optical region where the emission bands can be arranged in simple progression tables (Deslanders tables [9]), the vibrationally resolved x-ray or Auger spectra require in general an account of interference between the emitting levels due to the short lifetime of core ionized states [10–17]. This is described by the so-called lifetime-vibrational interference formula (LVI), which is nothing but the Kramers-Heisenberg dispersion relation assuming the Born-Oppenheimer and Condon approximations for the transition elements, and which has formed the common computational tool in the analysis of the spectra.

The possibility to resonantly excite x-ray and Auger emission [x-ray Raman scattering (RXS) spectra] has further promoted interest in the analysis of vibrational structure and nuclear dynamics in the x-ray region. New effects [5,18,6,19,8] relating the formation of the RXS spectral profile to the nuclear degrees of freedom have been discovered. Several of these refer to cases when dissociative states are involved and when both compound molecular and fragment signatures are identified in the spectra. Among several of these phenomena, for the purpose of the present work it is most relevant to mention a Doppler effect on ejected Auger electrons for core excitation above the dissociation threshold: The atomiclike resonance can be strongly influenced by such a Doppler effect as theoretically predicted [20] and experimentally confirmed [21] recently. On a closer inspection one finds that this Doppler effect is hidden in generalized Franck-Condon (GFC) amplitudes of the type [20]

$$\langle m|m_1\rangle \rightarrow \langle m|e^{i\varphi}|m_1\rangle, \quad \varphi = \pm\alpha \times \begin{cases} \mathbf{k}_{\mathrm{ph}} \cdot \mathbf{R} \\ \mathbf{k} \cdot \mathbf{R} \end{cases} \tag{1}$$

where α is connected with the reduced mass of the molecule. These photon- or electron-nuclear couplings originate in the photon and electron wave functions through the phase factors $\exp(i\varphi)$ that depend on the internuclear radius vector $\mathbf{R}$ and on the momenta of the x-ray photon, $\mathbf{k}_{\mathrm{ph}}$, or the photoelectron, $\mathbf{k}$. The GFC problem was only touched upon in Ref. [20] in connection with the special problem of computing the so-called atomiclike profile. In fact, as we show here, the GFC factors can significantly modify the whole RXS profile, thus also profiles for discrete vibrational transitions involving fully bound potentials, and also profiles for ordinary photoionization.

The aim of this paper is to present a general analysis of the role of the GFC amplitudes and factors in resonant x-ray-scattering spectra, especially for resonant photoemission where the photoelectron phase factors reflect the interference of electronic and nuclear motions and which leads to both important numerical corrections and additional spectral features. The GFC factors are shown to influence the RXS profile involving vibrational levels above and below the dissociation thresholds, that is, bound-bound transitions below or continuum-continuum transitions above the thresholds, or combinations thereof—continuum-bound and bound-continuum transitions. We show that the electron-vibrational profile of ordinary (direct) photoionization is also influenced by the GFC factors. The new spectral features caused by the GFC factors are expected to be the rule rather than the exception both in molecular photoionization and resonant photoemission.

*Permanent address: Institute of Automation and Electrometry, 630090 Novosibirsk, Russia.

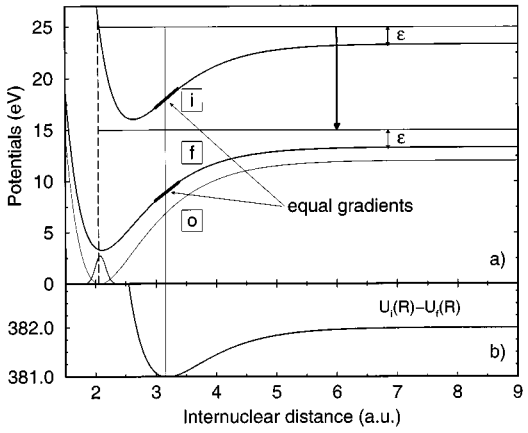

FIG. 1. Model interatomic potentials of the ground $[U_0(R)]$, core-excited $[U_i(R)]$, and final $[U_f(R)]$ states. The potentials of core-excited and final states are shifted: $U_i(R)-385\,\mathrm{eV}$, $U_f(R)-12\,\mathrm{eV}$. $\Delta U(R)=U_i(R)-U_f(R)$. The parameters of the potentials are collected in Table I.

II. PHYSICAL MODEL

We consider resonant x-ray scattering by molecules, i.e., scattering targets with nuclear degrees of freedom. The RXS process and energy scheme are illustrated in Fig. 1: The molecule in the ground state $|0\rangle$ first absorbs a photon of frequency ω and transits to the core excited states $|i\rangle$. These decay to the final states $|f\rangle$ by emission of the Auger electron with energy E [if not otherwise stated, the notation refers to nonradiative (Auger) scattering, although the theory is identical for radiative x-ray scattering].

A coherent picture is obtained by considering the Kramers-Heisenberg scattering amplitude [20]

$$F=\sum_{f,i}\frac{\langle f|Q|i\rangle\langle i|\mathcal{D}|0\rangle}{E-\omega_{if}+\imath\Gamma},\quad Q=qe^{\imath\mathbf{k}\cdot\mathbf{R}\alpha},$$
$$\mathcal{D}=(\mathbf{e}\cdot\mathbf{d})e^{\imath\mathbf{k}_{\mathrm{ph}}\cdot\mathbf{R}\alpha}. \tag{2}$$

Here $\mathbf{R}=\mathbf{R}_A-\mathbf{R}_B$ is the internuclear distance; $\alpha=\mu/m_A$, $\mu=m_Am_B/(m_A+m_B)$ is a reduced mass of the molecule; $\omega_{ji}=E_j-E_i$ is the resonant frequency of the electrovibrational transition $i\rightarrow j$; $\mathbf{e}$ is the polarization vector of incident photon with the frequency ω; $\mathbf{d}$ is the electronic transition dipole moment and q is the operator of the Auger decay in atom A; $\mathbf{k}_{\mathrm{ph}}$ and $\mathbf{k}$ are momenta of the x-ray photon and the photoelectron, respectively. Atomic units are used throughout the paper. Apparently, $Q=D'^{\dagger}$ in the case of radiative RXS (the emission of the final photon is marked by a prime). We pay attention in this paper mainly to the soft-x-ray regime; $\exp(i\mathbf{k}_{\mathrm{ph}}\cdot\mathbf{R}\alpha)\simeq 1$.

The RXS spectral properties are guided by the double differential cross section

$$\sigma(E,\omega)=|F|^2\Phi(E-\omega+\omega_{f0},\gamma), \tag{3}$$

where $\Phi(\Omega,\gamma)$ is the spectral function of an incident radiation. We restrict ourselves to the vibrational part of the problem and assume the Born-Oppenheimer (BO) approximation and also the Condon approximation insofar that all electronic transition matrix elements $q_{fi}(\mathbf{R})$ and $\mathbf{d}_{i0}(\mathbf{R})$ (but not the phase factors) can be extracted from the scattering amplitude (2). The evaluation of the RXS amplitude (2) is then reduced to the calculation of the generalized FC amplitudes

$$\langle f|Q|i\rangle\langle i|\mathcal{D}|0\rangle\simeq\langle f|q_{fi}(\mathbf{R})e^{-\imath\mathbf{k}\cdot\mathbf{R}\alpha}|i\rangle \times\langle i|[\mathbf{e}\cdot\mathbf{d}_{i0}(\mathbf{R})]e^{\imath\mathbf{k}_{\mathrm{ph}}\cdot\mathbf{R}\alpha}|0\rangle. \tag{4}$$

Now $|0\rangle$, $|i\rangle$, and $|f\rangle$ denote vibrational states of the ground, core-excited, and final electronic states, respectively. The dependence of $q_{fi}(\mathbf{R})$ and $\mathbf{d}_{i0}(\mathbf{R})$ on the nuclear coordinates can be important in general. For example, this is the case for transitions between highly excited or dissociative nuclear states with a large size of the nuclear wave function [22,23]. Another example is given by transitions near an avoided crossing of the potential surfaces where the electronic transition matrix elements depend strongly on $\mathbf{R}$ due to the strong dependence of mixing of the different electronic states on $\mathbf{R}$ [24,23,25]. However, very often the dependence of the electronic transition matrix elements on R can be neglected [26]. Both $q_{fi}(\mathbf{R})$ and $\mathbf{d}_{i0}(\mathbf{R})$ are assumed to be constant [26] in the following, and we focus on the role of the photon and photoelectron phase factors in Eq. (4), the new element of the theory. As mentioned above, it is of importance to keep only the photoelectron phase factor in the soft-x-ray region. This allows us to formulate the model

$$Q\rightarrow e^{\imath\mathbf{k}\cdot\mathbf{R}\alpha},\quad \mathcal{D}\rightarrow(\mathbf{e}\cdot\hat{\mathbf{d}}), \tag{5}$$

where $\mathbf{e}\cdot\hat{\mathbf{d}}$, with $\hat{\mathbf{d}}=\mathbf{d}/d$, is the polarization factor. One can interpret the appearance of the photoelectron phase term $\exp(-\imath\mathbf{k}\cdot\mathbf{R}\alpha)$ in the GFC amplitude (1) as the interference of the photoelectron with the nuclear motion.

We see that the profile of resonant photoemission in the soft-x-ray region is defined by the GFC amplitude $\langle f|Q|i\rangle$ for the Auger decay step and by the ordinary FC amplitude $\langle i|0\rangle$ for the photoabsorption step. We recall that the conventional theory of electron-vibrational bands in resonant photoemission is based on the assumption $Q=1$.

A. Time-dependent representation

To perform numerical simulations, we follow the time-dependent technique outlined in Ref. [27]. The previous studies [8] demonstrate that the temporal language allows a deeper insight into the physics of x-ray scattering, and the time-dependent techniques are also advantageous from the computational point of view. The RXS cross section $\sigma(E,\omega)$ can then be evaluated for arbitrary spectral distributions of incoming radiation $\Phi(\omega-\omega_1,\gamma)$ as the convolution [28–30,27]

$$\sigma(E,\omega)=\int d\omega_1\sigma_o(E,\omega_1)\Phi(\omega-\omega_1,\gamma),$$
$$\sigma_o(E,\omega)=\frac{1}{\pi}\mathrm{Re}\int_0^\infty d\tau\,\sigma_o(\tau)e^{i(\omega-E+E_o)\tau}. \tag{6}$$

This reduces the problem to an evaluation of the RXS cross section for monochromatic excitation $\sigma_o(E,\omega)$, which can be found in terms of the autocorrelation function [31,27]

TABLE I. Parameters of the Morse potentials, $U(R)=D_e[1-\exp(-(R-R_e)/a)]^2+E_0$, for ground, core-excited, and final states used in Fig. 1.

State	Vibrational frequency, ω_e (eV)	Anharmonicity, $\omega_e x_e$ (meV)	R_e (Å)	E_0 (eV)
Ground (o)	0.292	1.776	1.098	0
Core excited (i)	0.235	1.900	1.390	400.057
Final (f)	0.274	1.862	1.116	15.283

$$\sigma_o(\tau)=\langle\Psi(0)|\Psi(\tau)\rangle. \tag{7}$$

Here

$$|\Psi(\tau)\rangle=e^{-iH_f\tau}|\Psi(0)\rangle,$$

$$|\Psi(0)\rangle=\int_0^\infty dt\, e^{[\imath(\omega+E_0)-\Gamma]t}Q|\psi_i(t)\rangle. \tag{8}$$

The solution is obtained in two steps: (i) the solution of the Schrödinger equation in the core-excited state $i(\partial/\partial t)|\psi_i(t)\rangle=H_i|\psi_i(t)\rangle$ for $|\psi_i(t)\rangle=\exp(-iH_it)\mathcal{D}|o\rangle$ with the initial condition $|\psi_i(0)\rangle=\mathcal{D}|o\rangle$, and (ii) the solution of the Schrödinger equation for $|\Psi(\tau)\rangle$ with the final-state Hamiltonian H_f and with the initial condition $|\Psi(0)\rangle$. The physical meaning of the wave packets $|\psi_i(t)\rangle$ and $|\Psi(\tau)\rangle$ can be found in Refs. [32,27].

B. RXS spectral profile with ordinary FC amplitudes

We start from the examination of nonradiative RXS from the heteronuclear molecule with model potentials (Table I) shown in Fig. 1(a). In order to clearly see the role of the GFC amplitudes, we temporarily set aside the GFC effects and assume $Q=1$ (5). This leads to the well-known LVI (lifetime-vibrational interference) formula in the case of transitions involving bound potentials. In the case of resonant core excitation above the dissociation threshold [Fig. 1(a)], the simulated RXS spectrum consists of three qualitatively different parts; see Fig. 2. The left-hand side of the spectrum shows the extended sequence of narrow resonances which follow the Raman-Stokes dispersion law; this is the ''molecular band'' of continuum-bound transitions to the vibrational states of the final states. The right edge of the spectrum shown in the left panel of Fig. 2 corresponds to continuum-continuum transitions and is formed by two overlapping resonances; the broad M and the narrow A peaks (see also the right panel of Fig. 2). The peak position of resonance A does not depend on the excitation energy. The position of peak M deviates slightly from the constant value. As Fig. 1(a) indicates, peak A corresponds to the decay transitions in the dissociative region; it is the so-called atomiclike resonance following the non-Raman dispersion law [33,31]

$$E=\Delta U(\infty). \tag{9}$$

To understand the origin of peak M, let us compare Fig. 1(a) with the change, $\Delta U(R)=U_i(R)-U_f(R)$, of the core-excited state potentials involved [Fig. 1(b)]. It is clear that

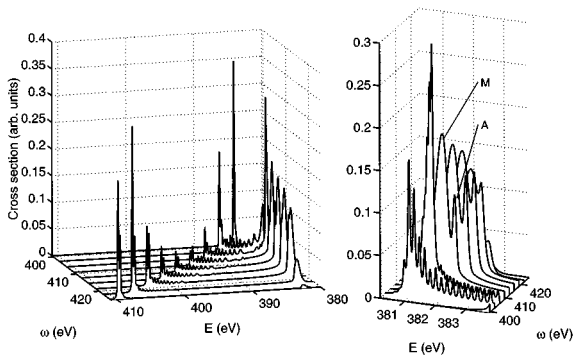

FIG. 2. The RXS cross section vs excitation energy without taking into account the photoelectron phase factor: $\exp(-\imath\mathbf{k}\cdot\mathbf{R}\alpha)\to 1$. The high-energy part of the spectrum (continuum-bound decays) follows to the Raman-Stokes law contrary to the low-energy part of the spectrum. The latter part (region near 380 eV) is caused mainly by continuum-continuum decay transitions. $\Gamma=0.065$ eV, $\Gamma_f=0.013$ eV, $m_A=m_B=14m_H$. The case of monochromatic excitation. $\omega_{i0}(\infty)=U_i(\infty)-E_0=407.2$ eV. The close-lying atomiclike resonance and molecular subband are denoted A and M, respectively.

the ''molecular'' continuum-continuum peak M is formed mainly near point R_c where the slope of $\Delta U(R)$ is equal to zero:

$$\frac{\partial}{\partial R}\Delta U(R)=0. \tag{10}$$

As in the dissociative region, and discussed earlier [see Eq. (23) in Ref. [31]], the decay transitions in the vicinity of this point occur with conservation of the kinetical energy of the relative nuclear motion. This results in a non-Raman dispersion relation for the peak position of the peak

$$E=\Delta U(R_c). \tag{11}$$

Apparently, this dispersion law is not strict due to the contribution to the resonance M from adjacent points, $R\neq R_c$, where the condition (10) breaks down. The result highlights nevertheless a new spectral feature of the molecular bands of RXS spectra, namely that one part (peak A) of the molecular bands follows the Raman-Stokes law, while the position of the other part (peak M) shows a very weak dependence on excitation frequency, Fig. 2.

III. RXS SPECTRAL PROFILE WITH GFC AMPLITUDES

A. GFC amplitudes for continuum-continuum and continuum-bound decay transitions. Doppler effects

For the generalization of the Franck-Condon factors, we reconsider first the case with core excitation above the dissociation threshold. Figure 3 displays the low-energy part of the RXS profile (Fig. 2) for the system shown in Fig. 1 and calculated with the GFC amplitudes. This part corresponds to the continuum-continuum decay transitions discussed above, consisting of two peaks, the broad molecular peak M and the narrow atomiclike peak A. Probably the most prominent new feature observed is the Doppler shift of the molecular peak M, Fig. 3(b); a Doppler shift of the atomiclike peak A was predicted [20] and observed [21] earlier. We remind the

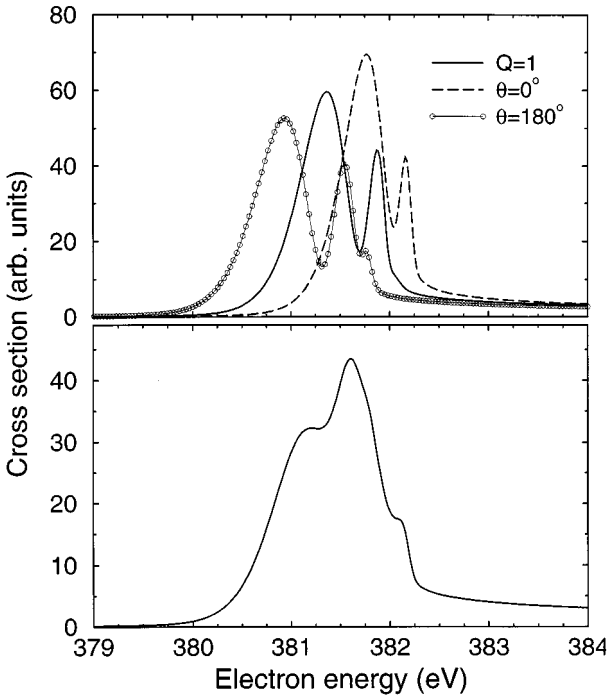

FIG. 3. The role of the GFC amplitudes on the RXS profile. $k=5.32$ a.u. $\mathbf{e}\|\mathbf{k}$. Core excitation to the unoccupied σ orbital. $\omega=408.8$ eV. (a) RXS from oriented molecules for different angles θ between $\mathbf{k}$ and molecular axis $\mathbf{R}$. (b) The RXS cross section averaged over molecular orientations. The orthogonal orientation of $\mathbf{k}$ and molecular axis ($\theta=90°$) correspond to the ordinary FC amplitudes with $Q=1$. Other parameters are the same as for Fig. 2.

reader that the Doppler shift, $\mathbf{k}\cdot\mathbf{v}$, is large due to a large velocity v of the dissociating atom and large momentum of the Auger electron. Figure 3(a) shows that the red and blue Doppler shifts result in different RXS profiles because of the influence of the smooth molecular background from the high-energy side of the A and M peaks.

The gas-phase molecules are oriented randomly and the RXS cross section must be averaged over molecular orientations. To be specific, we consider here core excitation to a σ unoccupied molecular orbital (MO). In such a case the photoabsorption factor $(\mathbf{e}\cdot\hat{\mathbf{d}}_{i0})^2$ (5) reads $\cos^2\theta$, where θ is the angle between $\mathbf{k}$ and the molecular axis. Figure 3(b) shows the smearing of the RXS profile due to the Doppler broadening. To see directly the role of the GFC amplitude, it is appropriate to compare Fig. 3(b) with Fig. 3(a) (solid line) showing the calculation with ordinary FC amplitudes. The high-energy part of the RXS spectrum (continuum-bound decays), Fig. 2, is not shown in Fig. 3. We note that the effect of the GFC amplitudes on the continuum-bound decays (Fig. 2) does not exceed 20%.

Doppler splitting and broadening of the atomiclike resonance

Very often the spacing between the atomiclike peak A and molecular peak M is large or peak M is absent [27]. In such a case one can examine the isolated atomiclike profile of RXS from oriented molecules: $\cos^2\theta/[(\Delta E-\mathcal{D}\cos\theta)^2+\Gamma^2]$. Here $\Delta E=E-\omega_\infty$, $\omega_\infty=\Delta U(\infty)=U_i(\infty)-U_f(\infty)$ represents the position of the atomiclike resonance, and $\mathcal{D}=kv$ is the Doppler shift. The final result of orientational

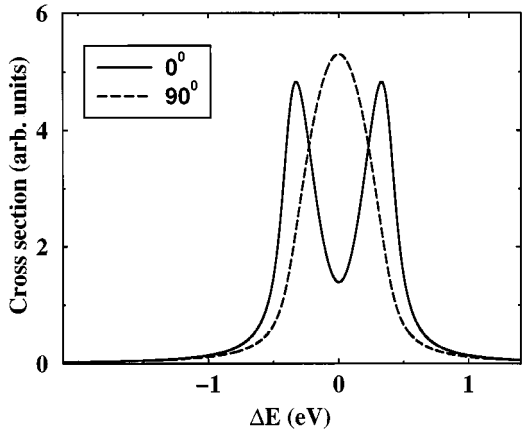

FIG. 4. The RXS profile for the isolated atomiclike resonance averaged over molecular orientations. Core excitation in the unoccupied σ orbital. The results of the simulations for $\vartheta=0°$ and 90° are based on Eq. (12). ϑ is the angle between $\mathbf{k}$ and $\mathbf{e}$. $\Gamma=0.09$ eV, $\mathcal{D}=0.4$ eV.

averaging is straightforward if we neglect the angular anisotropy of the Auger decay rate [21],

$$\sigma(E,\omega)=\sigma_\parallel(E,\omega)\cos^2\vartheta+\sigma_\perp(E,\omega)\sin^2\vartheta,$$

$$\sigma_\parallel(E,\omega)=\sigma_1+\left[\left(\frac{\Delta E}{\Gamma}\right)^2-1\right]\sigma_2,$$

$$\sigma_\perp(E,\omega)=\frac{1}{2}\left[\left(1+\frac{\mathcal{D}^2-\Delta E^2}{\Gamma^2}\right)\sigma_2-\sigma_1\right], \tag{12}$$

where

$$\sigma_1=\sigma_0\left(2+\frac{\Delta E}{\mathcal{D}}\ln\frac{(\Delta E-\mathcal{D})^2+\Gamma^2}{(\Delta E+\mathcal{D})^2+\Gamma^2}\right),$$

$$\sigma_2=\sigma_0\frac{\Gamma}{\mathcal{D}}\left[\arctan\left(\frac{\Delta E+\mathcal{D}}{\Gamma}\right)-\arctan\left(\frac{\Delta E-\mathcal{D}}{\Gamma}\right)\right]. \tag{13}$$

Here the RXS cross sections $\sigma_\parallel(E,\omega)$ and $\sigma_\perp(E,\omega)$ correspond to $\mathbf{k}\|\mathbf{e}$ and $\mathbf{k}\perp\mathbf{e}$, respectively; ϑ is the angle between $\mathbf{e}$ and $\mathbf{k}$. All unessential constants are collected in σ_0. Figure 4 shows, contrary to $\sigma_\perp(E,\omega)$, that $\sigma_\parallel(E,\omega)$ has two peaks which correspond to decay transitions in oppositely propagating atoms with opposite Doppler shifts. The reason for this is a partial alignment of the core-excited molecules. Indeed, molecules are oriented mainly parallel to the $\mathbf{e}$ vector under core excitation to unoccupied σ MO's. This results immediately in the Doppler splitting of the RXS profile when $\mathbf{k}\|\mathbf{e}$ [21] since in such a case the Auger electrons are ejected preferentially along the molecular axis; see Fig. 4.

When the Auger electron is emitted perpendicular to the molecular axis (which is oriented mainly along $\mathbf{e}$), the RXS profile collapses to a single broadened peak (see Fig. 4) since the Doppler shift is equal to zero in this case: $\mathbf{k}\cdot\mathbf{v}=\mathbf{0}$. One important difference between Fig. 3(b) and Fig. 4 deserves a comment. The Doppler splitting is not seen in Fig. 3(b) contrary to Fig. 4. The reason for this is the two-peak structure of the RXS profile shown in Fig. 3(a).

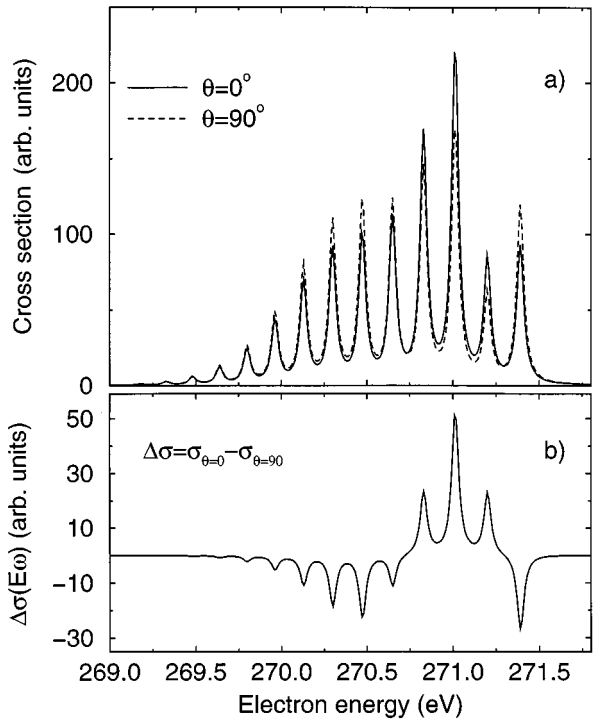

FIG. 5. The role of the GFC amplitudes under the bound-bound transition. The parameters of the potentials (of the ground $X^1\Sigma^+$, core excited $C\,1s^{-1}\pi^{*\,1}\Pi$, and final CO^+ $A\,^2\Pi$ states) for CO are from Ref. [37]. The case of nonradiative RXS from the oriented molecule CO. $\theta=0°$ and 90°. The orthogonal orientation of **k** and molecular axis ($\theta=90°$) corresponds to the ordinary FC amplitudes with $Q=1$. The lower panel (b) shows the difference $\Delta\sigma(E,\omega)$ of the RXS cross sections for $\theta=0°$ and $\theta=90°$. $\Gamma=0.0485$ eV, $\Gamma_f=0.013$ eV. The case of monochromatic excitation to the vibrational level $m=2$ of the core-excited state.

B. GFC amplitudes for bound-bound decay transitions

We examine vibrationally resolved bound-bound decay transitions below a dissociation threshold using core-excited $C\,1s^{-1}\pi^{*\,1}\Pi$ and final CO^+ $A\,^2\Pi$ states of the CO molecule as illustration. The molecular orientation is assumed to be along the Auger electron momentum **k** and $\mathbf{v}\perp\mathbf{k}$. Figure 5 shows that the effect of the GFC amplitudes on the direct bound-bound term in CO can be as large as 20%. This figure shows also the qualitative distinction of decay transitions to bound final states from the above-considered continuum-continuum decay transitions. One can see that the position of the resonances in the case of the bound final states does not depend on the phase factor (5), i.e., it does not experience a Doppler shift. It is not hard to understand that the role of the GFC increases when the effective size of the vibrational wave function increases. The interference of the photoelectron with a nuclear motion is thus enhanced near the dissociation threshold and for weakly bound ''van der Waals'' molecules like the sodium dimer or rare-gas halide molecules.

IV. ROLE OF THE GFC AMPLITUDES IN DIRECT PHOTOIONIZATION

We study the role of the GFC principle for direct x-ray photoionization by considering ionization from an occupied MO $\psi_i=c_{iA}\varphi_A+c_{iB}\varphi_B$ in a molecule *AB* to a continuum state with the electron momentum **k**. Here, φ_A and φ_B are atomic orbitals of atoms *A* and *B*. The electronic transition moment of photoionization reads in the one-electron approximation

$$\mathbf{d}_{io}\simeq c_{iA}\mathbf{d}_A e^{-\imath\alpha\mathbf{k}\cdot\mathbf{R}}+c_{iB}\mathbf{d}_B e^{\imath\beta\mathbf{k}\cdot\mathbf{R}}, \tag{14}$$

where $\beta=\mu/m_B$ and $\mathbf{d}_A$ is the atomic transition dipole moment. One can check that this expression is valid for a relatively high photoelectron energy, $kR\gtrsim 1$. The photoionization cross section can be expressed through the GFC amplitudes, $\langle i|\mathcal{D}(\mathbf{R})|0\rangle$, between vibrational wave functions $|0\rangle$ and $|i\rangle$ of ground and core-excited states,

$$\sigma_i(E,\omega)\propto\frac{|\langle i|\mathcal{D}(\mathbf{R})|0\rangle|^2}{(E-\omega-I_i-\nu_{i0})^2+\Gamma^2},$$

$$\mathcal{D}(\mathbf{R})=c_{iA}\mathcal{D}_A e^{-\imath\alpha\mathbf{k}\cdot\mathbf{R}}+c_{iB}\mathcal{D}_B e^{\imath\beta\mathbf{k}\cdot\mathbf{R}}. \tag{15}$$

Here $\mathcal{D}_A=(\mathbf{e}\cdot\mathbf{d}_A)$, I_i is the ionization potential of the MO level *i*, and ν_{i0} is the difference of vibrational energies of the excited and ground states. Averaging over molecular orientation leads to a strong suppression of the interference term between different atoms, $\propto 1/kR$. Making use of this, we immediately obtain

$$\sigma_i(E,\omega)\propto\int d\hat{\mathbf{R}}\frac{c_{iA}^2|\langle i|\mathcal{D}_A e^{\imath\alpha\mathbf{k}\cdot\mathbf{R}}|0\rangle|^2+c_{iB}^2|\langle i|\mathcal{D}_B e^{\imath\beta\mathbf{k}\cdot\mathbf{R}}|0\rangle|^2}{(E-\omega-I_i-\nu_{i0})^2+\Gamma^2}. \tag{16}$$

Apparently, the dependence of the GFC amplitudes on nuclear coordinates becomes essential when the photoelectron wavelength is comparable to (or shorter than) the effective size of the vibrational wave functions, ΔR:

$$k\,\Delta R\sim 1. \tag{17}$$

When this region is reached, one can expect a significant change of the vibrational profile with a further increase of excitation energy. It is worthwhile to mention that the GFC amplitude experienced by the photoelectron phase factors can be important in the formation of rotational bands of photoelectron spectra. Such resolution of the rotational structure has now become a reality, see, e.g., Refs. [34,35]. In some cases the amplitude of direct and resonant photoemission has the same order of magnitude and can therefore interfere. Clearly, the interference of direct and resonance terms is also influenced by the GFC amplitudes.

V. SUMMARY

With this paper we present the notion of a generalized Franck-Condon principle for the formation of spectral profiles in resonant photoemission. The generalized amplitudes differ from ordinary Franck-Condon amplitudes by the photoelectron phase factor, $\exp(-\imath\alpha(\mathbf{k}\cdot\mathbf{R}))$, in the integrand of the Kramers-Heisenberg expression for the scattering amplitude. The origin of the phase factor is the site selectivity of x-ray scattering caused by the strong localization of core

holes. The phase factor is changed during the molecular vibrations in a bound state or during the free molecular spread for excitation above the dissociation threshold. The variation of the phase factor results also in a numerical change of the FC amplitudes for vibrationally resolved bound-bound decay transitions. For example, the RXS cross section with the GFC amplitudes can differ from the cross section with the ordinary FC amplitudes up to approximately 20% for the CO molecule. This effect is enhanced for weakly bound ''van der Waals'' molecules with a large amplitude of vibrations.

The GFC amplitudes lead to qualitatively new spectral features in the RXS spectra under core excitation above the dissociation threshold, in particular to a Doppler effect for the ejected Auger electron associated to continuum-continuum transitions near the atomiclike resonance (large internuclear distance) [20]. This effect was recently observed in an experiment with O_2 molecules [21]. Here we found that the Doppler effect can influence also the continuum-continuum *molecular* band formed primarily due to decay transitions near the equilibrium geometry of the molecule. In contrast to the continuum-continuum band, the positions of the continuum-bound, bound-continuum, and bound-bound resonances are not influenced by Doppler shifts of the ejected electron.

The GFC amplitudes can be important also for photoelectron spectroscopy when the excitation energy exceeds the corresponding ionization threshold by several hundreds of eV's. In those cases one can expect a dependence of the vibrational band shape on the excitation energy due to the energy dependence of the GFC amplitudes.

The present work focuses on a generalization of the Franck-Condon principle; a further improvement of experimental-theoretical comparisons of resonant photoemission band profiles would be obtained by going beyond the Condon approximation and considering the variation of the Auger decay moments with geometry. Such calculations are now in progress [25,36].

ACKNOWLEDGMENT

This work was supported by the Swedish National Research Council (NFR).

[1] K. Siegbahn, C. Nordling, G. Johansson, J. Hedman, P. F. Hedén, K. Hamrin, U. Gelius, T. Bergmark, L. O. Werme, R. Manne, and Y. Baer, *ESCA Applied to Free Molecules* (North-Holland, Amsterdam, 1969).
[2] L. O. Werme, B. Grenberg, J. Nordgren, C. Nordling, and K. Siegbahn, Nature (London) **242**, 453 (1973).
[3] T. X. Carroll, S. E. Anderson, L. Ungier, and T. D. Thomas, Phys. Rev. Lett. **58**, 867 (1978).
[4] W. Eberhardt, in *Applications of Synchrotron Radiation*, edited by W. Eberhardt, Springer Series in Surface Sciences Vol. 35 (Springer-Verlag, Berlin, 1995), p. 203.
[5] J. Nordgren, J. Phys. IV **7**, C2-9 (1997).
[6] S. Svensson and A. Ausmees, Appl. Phys. A: Mater. Sci. Process. **65**, 107 (1997).
[7] M. N. Piancastelli, B. Kempgens, U. Hergenhahn, A. Kivimäki, K. Maier, A. Rüdel, and A. M. Bradshaw, Phys. Rev. A **59**, 1336 (1999).
[8] F. Gel'mukhanov and H. Ågren, Phys. Rep. **312**, 87 (1999).
[9] G. Herzberg, *Molecular Spectra and Molecular Structure. I. Spectra of Diatomic Molecules* (Van Norstrand, Princeton, 1950).
[10] F. Kh. Gel'mukhanov, L. N. Mazalov, and A. V. Kondratenko, Chem. Phys. Lett. **46**, 133 (1977).
[11] F. Kaspar, W. Domcke, and L. S. Cederbaum, Chem. Phys. **44**, 33 (1979).
[12] N. Correia, A. Flores-Riveros, H. Ågren, K. Helenelund, L. Asplund, and U. Gelius, J. Chem. Phys. **83**, 2035 (1985).
[13] T. X. Carrol, S. E. Anderson, L. Ungier, and T. D. Thomas, Phys. Rev. Lett. **58**, 867 (1987).
[14] A. Cesar, H. Ågren, and V. Carravetta, Phys. Rev. A **40**, 187 (1989).
[15] A. Cesar and H. Ågren, Phys. Rev. A **45**, 2833 (1992).
[16] R. Fink, J. Chem. Phys. **106**, 4038 (1997).
[17] S. K. Botting and R. R. Lucchese, Phys. Rev. A **56**, 3666 (1997).
[18] N. Mårtensson, M. Weinelt, O. Karis, M. Magnuson, N. Wassdahl, A. Nilsson, J. Stöhr, and M. Samant, Appl. Phys. A: Mater. Sci. Process. **65**, 159 (1997).
[19] B. Crasemann, Can. J. Phys. **76**, 251 (1998).
[20] F. Gel'mukhanov, H. Ågren, and P. Sałek, Phys. Rev. A **57**, 2511 (1998).
[21] O. Björneholm *et al.* (unpublished).
[22] K. Tamagake and D. W. Setser, J. Chem. Phys. **67**, 4370 (1977).
[23] K. F. Dunn, J. Geddes, F. P. O'Neill, N. Kouchi, and C. J. Latimer, J. Electron Spectrosc. Relat. Phenom. **79**, 373 (1996).
[24] J. Tellinghuisen, Adv. Chem. Phys. **60**, 299 (1985).
[25] R. F. Fink *et al.* (unpublished).
[26] H. Ågren, A. Cesar, and V. Carravetta, Chem. Phys. Lett. **139**, 145 (1987).
[27] P. Sałek, F. Gel'mukhanov, and H. Ågren, Phys. Rev. A **59**, 1147 (1999).
[28] F. Gel'mukhanov and H. Ågren, Phys. Rev. A **49**, 4378 (1994).
[29] Z. Gortel, R. Teshima, and D. Mentzel, Phys. Rev. A **58**, 1225 (1998).
[30] Z. Gortel and D. Mentzel, Phys. Rev. A **58**, 3699 (1998).
[31] F. Gel'mukhanov and H. Ågren, Phys. Rev. A **54**, 379 (1996).
[32] F. Gel'mukhanov, P. Sałek, T. Privalov, and H. Ågren, Phys. Rev. A **59**, 380 (1999).
[33] E. Kukk, H. Aksela, S. Aksela, F. Gel'mukhanov, H. Ågren, and S. Svensson, Phys. Rev. Lett. **76**, 3100 (1996).
[34] E. D. Poliakoff, H. C. Choi, R. M. Rao, A. G. Mihill, S. Kakar, K. Wang, and V. McKoy, J. Chem. Phys. **103**, 1773 (1995).
[35] G. Öhrwall, P. Baltzer, and J. Bozek, Phys. Rev. Lett. **81**, 546 (1998).
[36] V. Carravetta *et al.* (unpublished).
[37] S. Sundin, F. Gel'mukhanov, H. Ågren, S. J. Osborne, A. Kikas, O. Björneholm, A. Ausmees, and S. Svensson, Phys. Rev. Lett. **79**, 1451 (1997).